J|A|C|S
ARTICLES

Published on Web 07/06/2009

Photoelectron Spectroscopy of Lanthanide−Silicon Cluster Anions $LnSi_n^-$ ($3 \leq n \leq 13$; Ln = Ho, Gd, Pr, Sm, Eu, Yb): Prospect for Magnetic Silicon-Based Clusters

Andrej Grubisic, Yeon Jae Ko, Haopeng Wang, and Kit H. Bowen*

Departments of Chemistry and Materials Sciences, Johns Hopkins University, Baltimore, Maryland 21218

Received June 6, 2009; E-mail: kbowen@jhu.edu

Abstract: Photoelectron spectroscopy was utilized to study a variety of $LnSi_n^-$ cluster anions (Ln = Yb, Eu, Sm, Gd, Ho, Pr; $3 \leq n \leq 13$). For a particular size *n*, the measured valence electronic transitions of all these systems fall into either one of two categories, reflecting the influence of the different oxidation states of the lanthanide atoms involved. In one, the spectra of $YbSi_n^-$ and $EuSi_n^-$ are nearly identical to each other, while in the other the spectra of $GdSi_n^-$, $HoSi_n^-$, and $PrSi_n^-$ are essentially identical. $SmSi_n^-$ clusters exhibit an intermediate behavior with smaller clusters resembling the former category and larger clusters resembling the latter category. In the intermediate size range, $7 \leq n \leq 10$, for $SmSi_n^-$ both categories appear to be present, with one matching the $EuSi_n^-$-like systems and the other $HoSi_n^-$-like clusters. The distinction between $LnSi_n^-$ categories strongly correlates with the oxidation state of the particular lanthanide as usually found in its compounds. On the basis of this observation, we conclude that, among the Ln−silicon clusters studied herein, Yb, Eu, and in case of Sm, sizes $n \geq 10$, adopt a nominal +2 oxidation state while Ho, Pr, Gd, and in case of Sm, sizes $n \leq 7$, exhibit a nominal +3 oxidation state. Furthermore, dramatic increases in adiabatic electron affinity values observed at $n = 10$ for the $Ln^{III}Si_n$ series and at $n = 12$ for the $Ln^{II}Si_n$ series were attributed to an inherent electronic stabilization of those particular clusters, rather than to the lanthanides' encapsulation. The observed limited effect of f-electrons on the valence electronic structure and thus on bonding in $LnSi_n^-$ clusters may leave these electrons available for inducing magnetism. Consequently, $Ln@Si_n$ clusters may hold promise as building blocks of silicon-based cluster materials with magnetic properties.

Introduction

Small metal−silicon clusters have attracted considerable attention over the past two decades. The interest in part arises from the undeniable importance of silicon in the semiconductor industry. More importantly, however, the lion's share of that interest stems from the realization that the addition of "impurity" atoms can significantly alter the properties of silicon. For example, the notion of altering the electronic properties of silicon by doping group III (Ga, Al) and group V (P, As) elements into it has been in use for over half a century and has led to the revolutionary rise of modern computers. More recently, doping silicon microcrystals with erbium has been observed to drastically affect their optical properties.[1] With the discovery of the giant magnetoresistance (GMR) and the emergence of a nascent field of spintronics,[2,3] the focus has shifted to modifying silicon's magnetic properties as well.

The effects of an impurity atom are expected to be particularly pronounced when systems are composed of a small number of atoms (10−100). In this size regime the properties of the collective strongly depend on each and every constituent atom. Hence, even small changes, such as a substitution of an atom, can introduce significant changes in the cluster's chemical, electronic, magnetic, and optical properties. By using these clusters as building blocks, one can envision "designer" materials whose properties could be manipulated by fine-tuning the properties of their constituent clusters.

To obtain silicon-based building units for such materials, silicon cages have been considered as candidate motifs. Although empty silicon cages are not known to exist,[4] substantial experimental[5−11] and theoretical[12−24] work has shown that transition-metal (TM) atoms stabilize silicon cages by sitting endohedrally within them, $TM@Si_n$. Furthermore, it was concluded that several of these clusters, most notably $Ti@Si_{16}$, possess enhanced chemical stability that prevents them from aggregating when placed near one another.[11−13] Such systems provided encouraging markers on the path toward silicon-based cluster materials. What remained to be determined was which dopant atoms would impart silicon clusters with the desired properties.

In particular, if metal−silicon clusters were to exhibit magnetism, they might be able to serve as transitional materials between current silicon-based semiconductor technology and

(1) Kenyon, A. J. *Phil. Trans. R. Soc. London, A* **2003**, *361*, 345.
(2) Baibich, M. N.; Broto, J. M.; Fert, A.; Nguyen Van Dau, F.; Petroff, F.; Eitenne, P.; Creuzet, G.; Friederich, A.; Chazelas, J. *Phys. Rev. Lett.* **1988**, *61* (21), 2472.
(3) Binasch, G.; Grunberg, P.; Saurenbach, F.; Winn, W. *Phys. Rev. B* **1989**, *39* (7), 4828.
(4) Hudgins, R. R.; Imai, M.; Jarrold, M. F.; Dugourd, P. *J. Chem. Phys.* **1999**, *111* (17), 7865.

the nascent field of spintronics. Specifically, encapsulation of TM atoms into silicon cages was initially viewed as a promising venue for achieving this goal. Namely, unpaired d-electrons in TM atoms were envisioned as retaining their magnetic moments once encapsulated within a silicon cage. However, a considerable amount of evidence now shows that silicon's sp-orbitals interact strongly with the d-orbitals of the endohedral transition-metal atom, thereby quenching the latter's magnetic moment.[10,17,18] Because a nonzero magnetic moment arises from unpaired electrons and since a cluster's stability relies heavily on its ability to attain a closed shell, it becomes apparent why these two essential requirements for a magnetic cluster-assembled material are mutually exclusive when the same electrons are responsible for both bonding and magnetism.

To bypass this constraint, Khanna and Jena proposed the endohedral doping of silicon clusters with lanthanides (Ln). These elements are known to adopt relatively low oxidation numbers (from +2 to +4) in their compounds,[25] suggesting only limited participation of their f-electrons in bonding. Since the f-electrons are to a large extent not responsible for bonding, lanthanide atoms with multiple unpaired f-electrons may retain a significant portion of their atomic magnetic moments even in the presence of a strongly interacting environment such as a silicon cage. Decoupling of the electrons responsible for magnetism from those participating in bonding is therefore a crucial requirement for chemically stable, magnetic clusters.

Until recently, only a limited literature existed on lanthanide-containing silicon clusters. However, interest in their potential applications spurred considerable activity over the past couple of years. We have recently published the results of our experimental photoelectron spectroscopic studies of $EuSi_n^-$ ($3 \le n \le 17$)[26] and $GdSi_n^-$ ($2 \le n \le 13$)[27] cluster anions. Also, Ohara et al. had previously reported experimental photoelectron spectra and water reactivities of $TbSi_n^-$ ($6 \le n \le 16$).[28,29] Although offering only an indirect probe of the clusters' magnetism, when combined, these studies hint at likely magnetism of the Ln−silicon systems. Earlier theoretical work by Kumar et al. on encapsulated fullerene-like neutral and anionic clusters, $M@Si_{20}$ (M = La, Ac, Sm, Gd, Tm, Ce, Pa, Pu, Th, Np, Pm) had supported this implication. Specifically, their results indicated that $Pa@Si_{20}$, $Sm@Si_{20}$, $Pu@Si_{20}$, $Tm@Si_{20}$, and $Gd@Si_{20}^-$ retain rather significant magnetic moments in their most stable geometries.[30]

Here, we report the photoelectron spectra of several $LnSi_n^-$ cluster anion systems (Ln = Yb, Eu, Sm, Gd, Ho, Pr; $3 \le n \le 13$), thereby expanding the range of studied Ln−silicon systems to encompass half of the lanthanide series. For a given size n, similarities between the photoelectron spectra of two separate sets of $LnSi_n^-$ systems were observed. For example, the spectra of $EuSi_n^-$ and $YbSi_n^-$ are nearly identical, as are those of $GdSi_n^-$, $HoSi_n^-$, and $PrSi_n^-$. The absence of dopant atom-specific variations in the chemically relevant, valence, electronic structure indicates only limited involvement of the lanthanides' f-electrons in bonding with the silicon environment. This limited interaction with the neighboring silicon atoms implies that the f-electrons are left mostly unperturbed and are likely to remain largely as they were in an isolated Ln atom. In cases where some (or all) of a given lanthanide atom's f-electrons are unpaired, sizable magnetic moments may be found in their corresponding Ln−silicon clusters. Thus, while lacking direct measurements of their magnetic moments, these results nevertheless suggest potential for the existence of relatively stable, high-spin $LnSi_n^-$ clusters.

Experimental Methods

Anion photoelectron spectroscopy is conducted by crossing a beam of mass-selected negative ions with a fixed-frequency photon beam and energy-analyzing the resultant photodetached electrons. The photodetachment process is governed by the energy-conserving relationship $h\nu$ = EBE + EKE, where $h\nu$ is the photon energy, EBE is the electron binding energy, and EKE is the electron kinetic energy. Our apparatus has been described previously elsewhere.[31] Briefly, the apparatus consists of an ion source, a linear time-of-flight (TOF) mass analyzer, a Nd:YAG photodetachment laser, and a magnetic bottle (MB) photoelectron spectrometer. The instrumental resolution of the MB photoelectron spectrometer is ~35 meV at a 1 eV EKE. The fourth (266 nm, 4.661 eV) harmonic of a Nd:YAG was used to photodetach the cluster anions of interest. Photoelectron spectra were calibrated against the well-known atomic transitions of Cu^-.

Mixed lanthanide−silicon cluster anions were generated in a two-laser vaporization source, designed to mimic the arrangement first developed by Nakajima.[8] The details of our particular setup have been described elsewhere.[26] Briefly, two independent lasers ablate material from two different rods mounted on opposite sides of a horizontal channel. By tuning the laser power and the delay between the two laser pulses, one can control the amount as well as the composition of the generated plasma mixture. A correctly timed plume of ultra-high-purity helium propels the hot plasma mix down

(5) Beck, S. M. *J. Chem. Phys.* **1989**, *90* (11), 6306.
(6) Jaeger, J. B.; Jaeger, T. D.; Duncan, M. A. *J. Phys. Chem. A* **2006**, *110* (30), 9310.
(7) Janssens, E.; Gruene, P.; Meijer, G.; Woste, L.; Lievens, P.; Fielicke, A. *Phys. Rev. Lett.* **2007**, *99* (6), 063401.
(8) Koyasu, K.; Atobe, J.; Akutsu, M.; Mitsui, M.; Nakajima, A. *J. Phys. Chem. A* **2007**, *111* (1), 42.
(9) Ohara, M.; Koyasu, K.; Nakajima, A.; Kaya, K. *Chem. Phys. Lett.* **2003**, *371* (3−4), 490.
(10) Zheng, W.; Nilles, J. M.; Radisic, D.; Kit H Bowen, J. *J. Chem. Phys.* **2005**, *122* (7), 071101.
(11) Hiura, H.; Miyazaki, T.; Kanayama, T. *Phys. Rev. Lett.* **2001**, *86* (9), 1733.
(12) Kumar, V.; Kawazoe, Y. *Phys. Rev. Lett.* **2001**, *87* (4), 045503.
(13) Miyazaki, T.; Hiura, H.; Kanayama, T. *Phys. Rev. B* **2002**, *66* (12), 121403.
(14) Hagelberg, F.; Xiao, C.; Lester, W. A. *Phys. Rev. B* **2003**, *67* (3), 035426.
(15) Han, J.-G.; Shi, Y.-Y. *Chem. Phys.* **2001**, *266* (1), 33.
(16) Jackson, K.; Nellermoe, B. *Chem. Phys. Lett.* **1996**, *254* (3−4), 249.
(17) Khanna, S. N.; Rao, B. K.; Jena, P. *Phys. Rev. Lett.* **2002**, *89* (1), 016803.
(18) Khanna, S. N.; Rao, B. K.; Jena, P.; Nayak, S. K. *Chem. Phys. Lett.* **2003**, *373* (5−6), 433.
(19) Kumar, V. *Comput. Mater. Sci.* **2004**, *30* (3−4), 260.
(20) Kumar, V. *Comput. Mater. Sci.* **2006**, *35* (3), 375.
(21) Kumar, V. *Comput. Mater. Sci.* **2006**, *36* (1−2), 1.
(22) Kumar, V.; Majumder, C.; Kawazoe, Y. *Chem. Phys. Lett.* **2002**, *363* (3−4), 319.
(23) Reveles, U. J.; Khanna, S. N. *Phys. Rev. B* **2006**, *74* (3), 035435.
(24) Sen, P.; Mitas, L. *Phys. Rev. B* **2003**, *68* (15), 155404.
(25) Greenwood, N. N.; Earnshaw, A., *Chemistry of the Elements*, 2nd ed.; Butterworth-Heinemann: Oxford, U.K., Boston, 1997.
(26) Grubisic, A.; Wang, H.; Ko, Y. J.; Bowen, K. H. *J. Chem. Phys.* **2008**, *129* (5), 054302.
(27) Grubisic, A.; Wang, H.; Ko, Y. J.; Stokes, S. T.; Zheng, W.; Li, X.; Bowen, K. H. Photoelectron Spectroscopy of Gadolinium-Silicon Mixed Cluster Anions $GdSi_n^-$ ($2 \le n \le 13$): Limited Participation of Electrons in Bonding Leaves Them Available for Magnetism. In press.
(28) Ohara, M.; Miyajima, K.; Pramann, A.; Nakajima, A.; Kaya, K. *J. Phys. Chem. A* **2002**, *106* (15), 3702.
(29) Ohara, M.; Miyajima, K.; Pramann, A.; Nakajima, A.; Kaya, K. *J. Phys. Chem. A* **2007**, *111* (42), 10884.
(30) Kumar, V.; Singh, A. K.; Kawazoe, Y. *Phys. Rev. B* **2006**, *74* (12), 125411.

the exit channel of the source, thereby cooling the ablated material and forming clusters.

For this particular set of experiments, a silicon rod (1/4 in. diameter, 3N5 purity, purchased from ESPI) was positioned downstream and ablated with 532 nm laser light from a Nd:YAG laser. As the source of the lanthanide element, a 1/4 in. diameter rod was employed in the case of praseodymium (3N purity, purchased from ESPI), whereas in the case of the other lanthanides a foil (25 × 25 mm, 0.010′ in. thick, 3N purity, purchased from Alfa Aesar) wrapped around an aluminum mandrel was used to act as a lanthanide "rod". This rod was ablated by a mixture of 1064 and 532 nm light from a second Nd:YAG laser that lacked the dichroic mirrors to separate the two harmonics. To improve the stability of the mixed cluster intensities, a stable shot-to-shot behavior of this laser had to be ensured. To achieve this, an attenuator was utilized to reduce the laser's power output from a high value, where the laser exhibits its best shot-to-shot stability, to a low value required for best mixed cluster generation. For optimal mixing, the laser pulse hitting the silicon rod was delayed by ~5 μs relative to the one ablating the lanthanide element.

Results

Figure 1 shows typical mass spectra of some representative $LnSi_n^-$ cluster anion series generated from our source, when it was optimized for the highest yield of the single lanthanide atom-containing species. The insets show selected magnified portions of the mass spectra, revealing the expected isotope patterns. $HoSi_n^-$ clusters are ideally suited for mass-selected studies because holmium exists as a single isotope and possesses an atomic mass that is several mass units removed from the nearest Si_n^- cluster, thereby avoiding a direct mass coincidence (Figure 1a). A similar situation is encountered in the case of $EuSi_n^-$ clusters (see the mass spectrum in ref 26) because europium has few isotopes as well (i.e., 2). The advantage of fewer isotopes becomes apparent upon viewing the mass spectra of $SmSi_n^-$ (Figure 1b) and $GdSi_n^-$ (see the mass spectrum in ref 27) species. Both lanthanides have seven naturally occurring isotopes that extend over a ~10 amu mass range, leading to broad mass distributions of individual $LnSi_n^-$ clusters. Although they avoid a direct mass coincidence with the Si_n^- series, they do overlap with tails of even broader distributions from members of $Ln_{m>1}Si_n^-$ series. The mass overlaps of these multiple lanthanide atom-containing silicon clusters can be substantial, especially when studying larger $LnSi_n^-$ ($n \geq 15$) systems. While $PrSi_n^-$ clusters (Figure 1c) have the advantage of containing a lanthanide element that has a single isotope, their mass coincidence with Si_n^-, and consequently with the $Pr_{m>1}Si_n^-$ series, prevents one from isolating clusters with a unique composition. Although a full separation of different clusters is impossible in such cases, optimizing the source conditions to preferentially produce the desired cluster series was exploited to obtain predominantly those compositions that we wished to probe. This method was utilized to obtain relatively well-isolated $PrSi_n^-$ clusters ($n \leq 9$). In the case of the $YbSi_n^-$ series (Figure 1d) the situation is further complicated not only by their partial mass coincidence with the Si_n^- clusters, but also by broadened mass distributions due to seven isotopes of ytterbium. Nevertheless, relatively pure compositions for $YbSi_n^-$ ($n \leq 13$) were obtained with careful attention to the source conditions.

Photoelectron spectra of all studied $LnSi_n^-$ (Ln = Ho, Gd, Pr, Sm, Eu, Yb) systems are presented in Figure 2. On the basis of their appearance, the lanthanide−silicon systems can be categorized as belonging either in one of two distinct classes or in one intermediate class. Members within each class exhibit nearly identical photoelectron spectral signatures. Spectra of Eu and Yb fall into category "A" and are distinguished by a low EBE feature observed for sizes $n \leq 12$. Photoelectron spectra of Ho, Gd, and Pr species generally differ from those of category A members, with their most characteristic distinction being the lack of comparably low EBE peaks. These elements belong to category "B". Sm was categorized in an intermediate category of its own, "AB", because the spectra of smaller $SmSi_n^-$ ($n \leq 6$ and $n = 9$) clusters resemble those of category A members with the same n, while the spectra of larger $SmSi_n^-$ ($n \geq 11$) clusters look more like those of category B members. Interestingly, the spectra of $SmSi_7^-$, $SmSi_8^-$, and $SmSi_{10}^-$ appear to display features that are a combination of the two. This is demonstrated in Figure 3, where the summation of appropriately scaled photoelectron spectra of two prototypical members of each category ($EuSi_n^-$ for category A and $HoSi_n^-$ for category B) yields approximately the overall spectrum of a particular $SmSi_n^-$ cluster. It was furthermore observed that, by varying the source conditions, their relative contributions to the overall spectral profile changed. An example of such variations is demonstrated in Figure 4 for the case of $SmSi_{10}^-$. The result

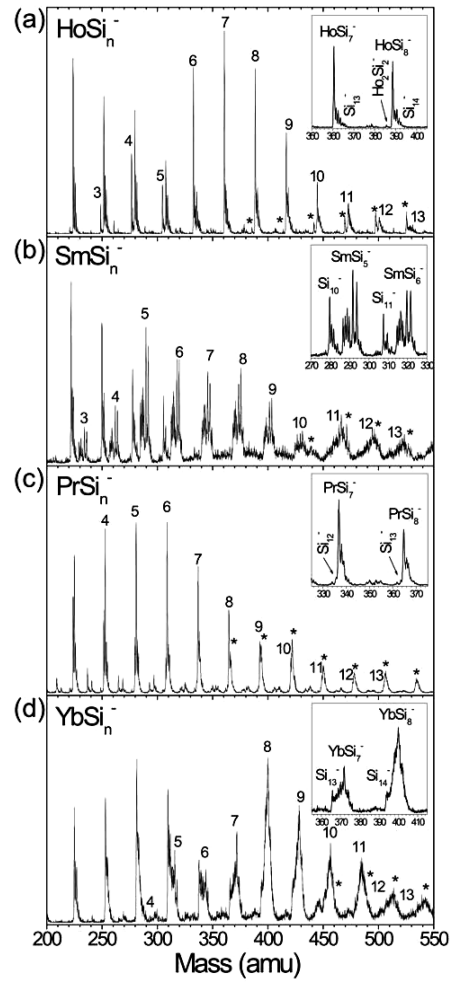

Figure 1. Typical anion mass spectra of mixed Ln−Si clusters obtained from a two-laser vaporization source that was optimized for production of single lanthanide atom-containing clusters: (a) $HoSi_n^-$; (b) $SmSi_n^-$; (c) $PrSi_n^-$; (d) $YbSi_n^-$. Silicon clusters containing two lanthanide atoms are marked with an asterisk. The insets show selected magnified portions of the mass spectra, revealing the expected isotope patterns.

(31) Gerhards, M.; Thomas, O. C.; Nilles, J. M.; Zheng, W.-J.; Bowen, K. H. *J. Chem. Phys.* **2002**, *116* (23), 10247.

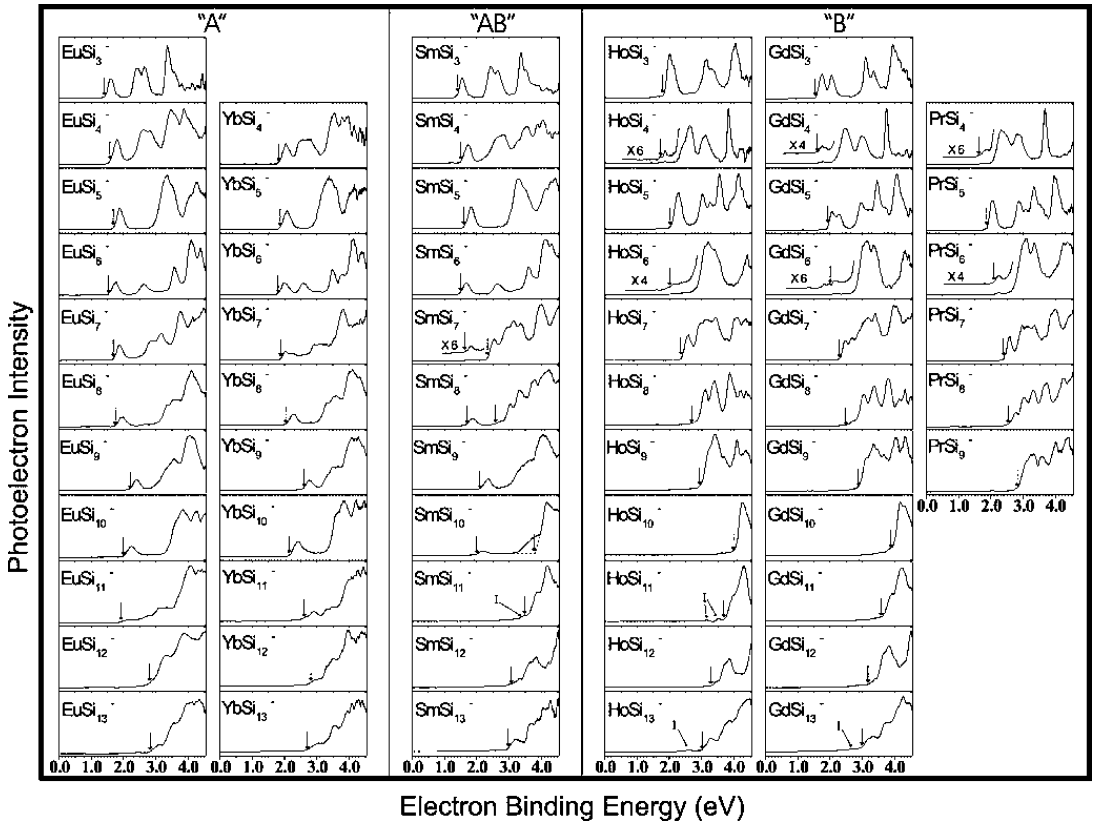

Figure 2. Photoelectron spectra of $LnSi_n^-$ ($3 \leq n \leq 13$) cluster anions recorded with 266 nm photons. The vertical arrows indicate the threshold energies from which the adiabatic electron affinities (EA_a) of the corresponding $LnSi_n$ clusters were inferred. Due to the presence of two isomers for $SmSi_n^-$ ($n = 7, 9, 10$) two vertical arrows are drawn in their photoelectron spectra approximately pointing at the threshold energies of each isomer. Peaks corresponding to an impurity are marked with "I".

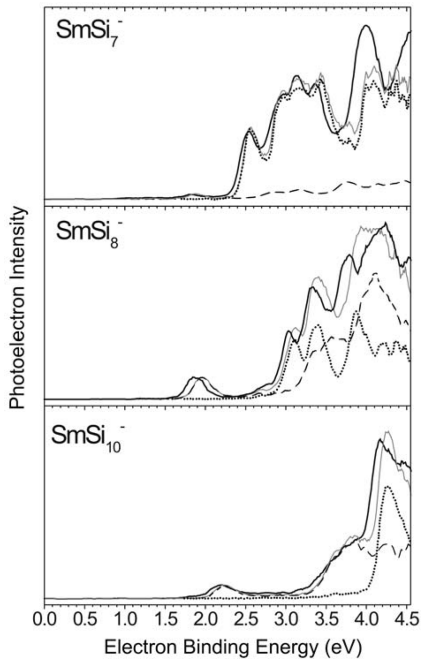

Figure 3. Photoelectron spectra of (a, top) $SmSi_7^-$, (b, middle) $SmSi_8^-$, and (c, bottom) $SmSi_{10}^-$ (solid black) deconvoluted into contributions from a category A-like, i.e., $EuSi_n^-$ (dashed), and category B-like, i.e., $HoSi_n^-$ (dotted), system. Aside from the small systematic shift of the individual spectra, the overall spectrum of a particular $SmSi_n^-$ (gray solid) can be reasonably reproduced by scaling the spectra of $EuSi_n^-$ and $HoSi_n^-$ at the same n.

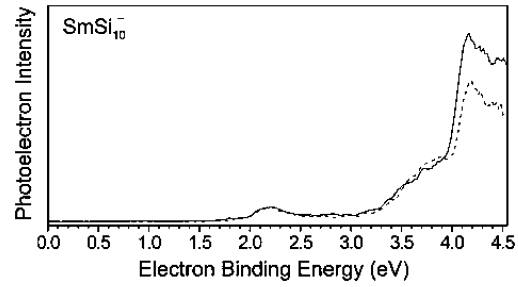

Figure 4. Photoelectron spectrum of $SmSi_{10}^-$ recorded with 266 nm photons at two different sets of source conditions.

implies that the observed spectral superposition is a consequence of the presence of two different isomers. It further suggests that the two isomers are similar to those encountered in the case of category A and B members. The absence of similarly obvious changes in the case of $SmSi_8^-$ and $SmSi_9^-$ hints that, within each of these isomer pairs, the two cluster species are energetically nearly degenerate.

While the photoelectron spectra within each category are nearly identical, there are some differences. Among the category A members, the spectrum of $EuSi_{11}^-$ exhibits a tail in the EBE range of 1.9−2.7 eV, which is absent in the case of $YbSi_{11}^-$. Furthermore, a well-defined gap between the lowest EBE peaks in the spectrum of $EuSi_7^-$ is congested with transitions in the case of $YbSi_7^-$. For small cluster sizes, $n \leq 10$, the spacing between the two lowest energy transitions in the case of $YbSi_n^-$ is generally smaller than either in $EuSi_n^-$ or in category A-like $SmSi_n^-$ clusters ($n \leq 6$, $n = 9$). Among members of category

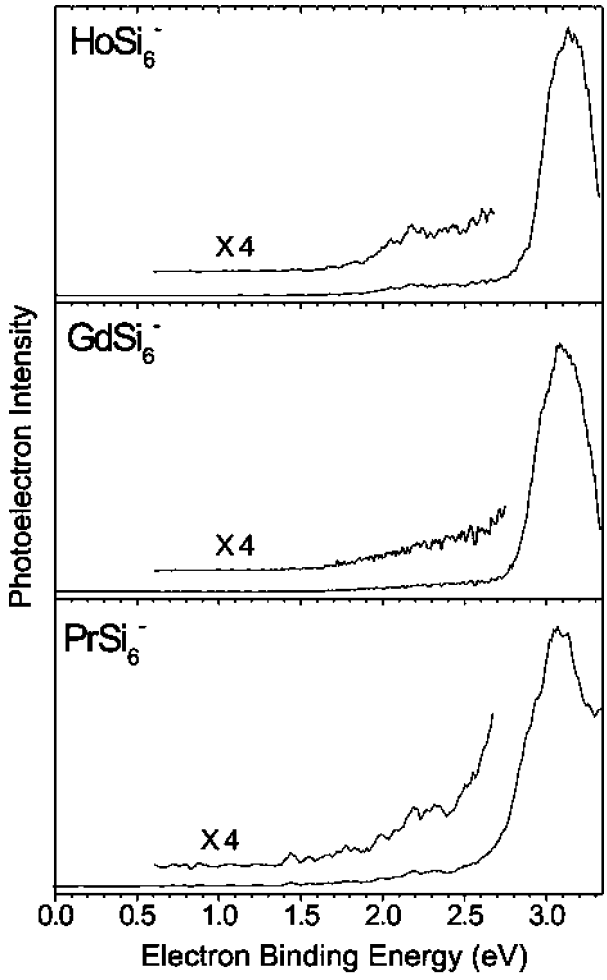

Figure 5. Photoelectron spectra of (a, middle) $GdSi_6^-$, (b, top) $HoSi_6^-$, and (c, bottom) $PrSi_6^-$ recorded with 355 nm photons.

B, the most conspicuous difference is the enhanced splitting of the lowest energy feature in the case of smaller, odd-numbered $GdSi_n^-$ systems ($n = 3, 5, 7$). In addition, for $n = 8$ a well-defined peak at ~2.7 eV in the spectrum of $PrSi_8^-$ decreases in intensity in the case of $GdSi_8^-$ and in the category B-like isomer of $SmSi_8^-$ until it almost completely disappears in the spectrum of $HoSi_8^-$.

An interesting spectral shape is observed for $LnSi_6^-$ when Ln belongs to category B. In these cases a weak plateau in photoelectron intensity is observed that begins at ~1.8 eV and extends up to the threshold of the first strong feature that peaks at ~3 eV. This plateau appears not to change in intensity relative to the larger peak upon repeated measurements and is observed in spectra recorded with 266 nm photons (Figure 2) as well as with 355 nm photons (Figure 5). In addition, the previously reported spectrum of $TbSi_6^-$ reveals a similar, even slightly more pronounced, tail in this region.[28,29] Together, the evidence suggests that the photoelectron intensity in this part of the spectrum is not due to an impurity, an isomer, or a series of hot bands, but is rather an integral part of the electronic structure of the $LnSi_6^-/LnSi_6$ system.

In contrast to bare Si_n^- clusters, the photoelectron spectra of $LnSi_n^-$ clusters at the same n generally exhibit more and usually sharper transitions.[32−37] In that regard, $LnSi_n^-$ clusters more closely resemble $(TM)Si_n^-$ systems. However, their spectral patterns are observed to depend to a much lesser extent on the identity of the dopant atom than is the case among the $(TM)Si_n^-$ systems. There, nearly every system containing a different TM element is found to exhibit a unique spectral fingerprint at a given size n.[8]

Discussion

Peaks in anion photoelectron spectra correspond to transitions from the ground electronic state of the anion to the ground and excited electronic states of its corresponding neutral. Consequently, anion photoelectron spectroscopy provides information on not only the anion, but also the electronic structure of the neutral species. Additionally, by probing only the outermost energy levels, UV/vis photoelectron spectroscopy tracks changes precisely in those valence orbitals that are responsible for bonding within a particular system. Therefore, if the substitution of an atom in a cluster influences its bonding, differences in the appearance of the photoelectron spectra should be observable. On the other hand, the absence of such variations would imply that the bonding in the studied systems is similar if not identical.

The observation that the photoelectron spectra of $LnSi_n^-$ clusters can be grouped according to their similar spectral appearances therefore indicates that bonding within the clusters from the same category is largely unaffected by the exchange of a lanthanide atom. Since the valence energy levels probed by the photoelectron spectroscopy reflect not only how the cluster is bonded within, but also how it interacts with its surroundings, it can be inferred that the chemical properties of clusters in the same category are also nearly identical. Thus, $EuSi_n^-$ and $YbSi_n^-$ (category A), which exhibit nearly identical spectra, can be considered chemically analogous. The same is true among the $GdSi_n^-$, $HoSi_n^-$, and $PrSi_n^-$ systems (category B). Since the photoelectron spectra of these latter systems also resembled previously reported spectra of the $TbSi_n^-$ series,[28,29] we conclude that Tb behaves like a member of category B as well. On the other hand, $SmSi_n^-$ (category AB) clusters switch from being category A-like in small clusters ($2 \le n \le 6$, $n = 9$) to being category B-like at larger sizes ($n \ge 11$). For clusters with intermediate behavior ($n = 7, 8, 10$), it is observed that they are actually a mixture of two different isomers with one belonging to category A and the other to category B. Overall, therefore, it appears that, among all the studied systems, for the same n, there exist only two chemically distinct structures that differ in their spectral fingerprints. One set of structures are represented by the members of category A and the other by members of category B. Moreover, the clusters from the same category are chemically nearly identical regardless of the choice of the lanthanide, provided that n stays the same. The observed

(32) Bai, J.; Cui, L.-F.; Wang, J.; Yoo, S.; Li, X.; Jellinek, J.; Koehler, C.; Frauenheim, T.; Wang, L.-S.; Zeng, X. C. *J. Phys. Chem. A* **2006**, *110* (3), 908.
(33) Cheshnovsky, O.; Yang, S. H.; Pettiette, C. L.; Craycraft, M. J.; Liu, Y.; Smalley, R. E. *Chem. Phys. Lett.* **1987**, *138* (2−3), 119.
(34) Maus, M.; Ganteför, G.; Eberhardt, W. *Appl. Phys. A: Mater. Sci. Process.* **2000**, *70*, 535.
(35) Meloni, G.; Ferguson, M. J.; Sheehan, S. M.; Neumark, D. M. *Chem. Phys. Lett.* **2004**, *399* (4−6), 389.
(36) Muller, J.; Liu, B.; Shvartsburg, A. A.; Ogut, S.; Chelikowsky, J. R.; Siu, K. W. M.; Ho, K.-M.; Gantefor, G. *Phys. Rev. Lett.* **2000**, *85* (8), 1666.
(37) Xu, C.; Taylor, T. R.; Burton, G. R.; Neumark, D. M. *J. Chem. Phys.* **1998**, *108* (4), 1395.

limited effect of the identity of the lanthanide atom on the chemical properties of the $LnSi_n^-$ clusters therefore implies that the f-electrons are, to a large extent, not responsible for bonding within these clusters.

In chemistry, oxidation numbers serve as a qualitative indicator of the degree to which the element's valence electrons participate in bonding with the environment. The apparent lack of a significant effect by the f-electrons on the valence electronic structure of $LnSi_n^-$ clusters belonging to the same category therefore suggests that those lanthanide atoms adopt the same oxidation numbers. Interestingly, a strong correlation exists between the oxidation numbers that a particular lanthanide adopts in its oxides and fluorides[25] and the $LnSi_n^-$ category to which a given lanthanide belongs. For example, Eu and Yb, members of category A, often exhibit the +2 oxidation state. This is rationalized by the extra stability that these two lanthanides achieve upon donation of their two valence s-electrons, which gives rise to half-filled and completely filled f-electron shells, respectively (Eu, $[Xe]6s^24f^7$; Yb, $[Xe]6s^24f^{14}$). On the other hand, Gd ($[Xe]6s^24f^75d^1$) and Ho ($[Xe]6s^24f^{11}$), members of category B, are predominantly found in the +3 oxidation state. Although Pr ($[Xe]6s^24f^3$) and Tb ($[Xe]6s^24f^9$) are known to exist in +3 and +4 oxidation states, the similarity between their photoelectron spectra and those of category B members suggests that in these clusters they prefer to take on the +3 oxidation state as well. Furthermore, the peculiar behavior of $SmSi_n^-$ systems is consistent with the observation that Sm ($[Xe]6s^24f^6$) is commonly found in both +2 and +3 oxidation states in its compounds. In smaller $SmSi_n^-$ clusters ($n \leq 6$), which resemble members of category A, we conclude that Sm is in the +2 oxidation state. The strengthening interaction with the growing number of silicon atoms in the cluster causes the oxidation number on Sm to change from +2 to +3 in the range over $n = 8-10$. By size $n = 11$, Sm in $SmSi_n^-$ is predominantly in the +3 oxidation state. Interestingly, $SmSi_7^-$ stands out as being the smallest cluster in which the Sm atom almost completely adopts a +3 state. Therefore, the evidence suggests that the lanthanides in $LnSi_n^-$ systems belonging to category A adopt the +2 oxidation state and those in clusters belonging to category B take on the +3 oxidation number. It is interesting to note that the lanthanides exhibit the same kind of behavior in the strongly interacting environment of silicon as has been previously observed in the relatively weakly interacting Ln−cyclooctatetraene (COT)[38,39] and Ln@fullerene systems.[40] This implies that the lanthanides' f-electronic levels reside deep within the Ln atoms' electronic cores, where even a strong perturbation from their surroundings does not significantly affect them.

The observed limited participation of f-electrons in bonding of lanthanide atoms in $LnSi_n^-$ clusters enhances the prospects for magnetic lanthanide−silicon-based materials. By avoiding significant perturbation from the silicon environment, the f-electrons of lanthanides stand in stark contrast to the d-electrons of the transition-metal atoms. There, the unpaired d-electrons are known to strongly interact with the silicon cage by forming chemical bonds, thereby quenching their magnetic moments. The differing behavior of the lanthanides therefore gives rise to the possibility that the isolated lanthanide atom's unpaired f-electrons remain unpaired when placed into a silicon environment, thereby leading to significant magnetic moments in Ln−silicon clusters. Interestingly, such magnetism was detected in various Ln@fullerene and Ln−COT systems.[40,41] In the latter case, the photoelectron spectra of various $(Ln-COT)^-$ systems were as similar to each other as were those of the $LnSi_n^-$ systems discussed in this paper,[38] corroborating the hypothesis that the Ln−silicon clusters remain magnetic as well. An additional reason for optimism comes from a study of $Ba_6Ce_2Au_4Si_{42}$ clathrate-like material, where Ce atoms were found to occupy the endohedral sites of the Si_{20} cages within the alloy and to exhibit a magnetic moment of 0.8 μ_B per atom.[42] Note that an isolated Ce atom has only one f-electron and that the other lanthanides may give rise to even larger magnetic moments.

From a quantum chemical standpoint the implications of such potentially closed-shell materials with magnetic properties are quite intriguing. The absence of significant changes in the valence energy levels of Ln−silicon clusters upon substitution of a lanthanide atom (that prefers the same oxidation state) suggests that the f-levels are buried deeper within the electronic energy structure than the chemically relevant ~0−2 eV range that was probed. If they had not been, the varying population of the f-electrons would have been observable as changing photoelectron spectral signatures for different $LnSi_n^-$ clusters. Furthermore, since the f-shell was, except for Yb, only partially filled, the lack of reorganization in the population of the clusters' valence energy levels implies that empty f-states remain below the occupied valence states. This apparent violation of the Aufbau principle turns out not to be unique to these systems, but is often encountered in systems where bonding has a significant ionic character, e.g., transition-metal oxides.[43] If Ln−silicon species were to exhibit significant ionic character, electron transfer from the lanthanide atom to the silicon moiety would give rise to species such as $Ln(II)^{2+}(Si_n)^{2-}$ and $Ln(III)^{3+}(Si_n)^{3-}$, and in a potential material, this would be manifested as a Zintl-like salt.[44]

The separation of electrons responsible for bonding and chemical properties of a cluster from those accountable for their magnetic characteristics allows for independent tuning of the two sets of properties, both of which are essential for developing a chemically stable, magnetic cluster-assembled material. By comparison, another promising class of clusters, $TM@X_{10}^{2-}$ and $TM@X_{12}^{2-}$ (X = Sn, Pb),[45,46] relies on their highly symmetrical structure to attain magnetic properties. There, the symmetry gives rise to substantial degeneracy of their outermost valence energy levels, leading to high-spin, open-shell species which are magnetic, but which may also be chemically reactive. While geometry plays a crucial role in determining the magnetic properties of $TM@X_{10}$ and $TM@X_{12}$ clusters, it appears to play only a minor role in affecting the magnetic properties of the Ln−silicon clusters. Structural aspects, however, do exert a significant influence on the suitability of a particular cluster as a building block of a cluster-based material.

(38) Kurikawa, T.; Negishi, Y.; Hayakawa, F.; Nagao, S.; Miyajima, K.; Nakajima, A.; Kaya, K. *J. Am. Chem. Soc.* **1998**, *120* (45), 11766.
(39) Takegami, R.; N, N. H.; Suzumura, J.; Nakajima, A.; Yabushita, S. *J. Phys. Chem. A* **2005**, *109* (11), 2476.
(40) Shinohara, H. *Rep. Prog. Phys.* **2000**, *63*, 843.
(41) Miyajima, K.; Knickelbein, M. B.; Nakajima, A. *J. Phys. Chem. A* **2008**, *112* (3), 366.
(42) Kawaguchi, T.; Tanigaki, K.; Yasukawa, M. *Phys. Rev. Lett.* **2000**, *85* (15), 3189.
(43) Merer, A. J. *Annu. Rev. Phys. Chem.* **1989**, *40*, 407.
(44) Zintl, E. *Angew. Chem.* **1939**, *52*, 1.
(45) Esenturk, E. N.; Fettinger, J.; Eichhorn, B. *J. Am. Chem. Soc.* **2006**, *128*, 9178.
(46) Cui, L.-F.; Wang, L.-S. *Int. Rev. Phys. Chem.* **2008**, *27* (1), 139.

Table 1. Estimated Adiabatic Electron Affinities, EA_a, of $LnSi_n$ Clusters Inferred from the Photoelectron Spectra of $LnSi_n^-$ Clusters (Figure 2)

	EA_a (eV)				
n ($LnSi_n$)	$YbSi_n$	$SmSi_n$[a]		$HoSi_n$	$PrSi_n$
3		1.40 ± 0.05		1.85 ± 0.05	
4	1.80 ± 0.05	1.50 ± 0.05		1.7 ± 0.1	1.6 ± 0.1
5	1.85 ± 0.05	1.60 ± 0.05		2.05 ± 0.05	1.9 ± 0.1
6	1.80 ± 0.05	1.5 ± 0.1		2.0 ± 0.2	2.1 ± 0.1
7	1.85 ± 0.05	1.6 ± 0.1	2.35 ± 0.05	2.4 ± 0.1	2.4 ± 0.1
8	2.05 ± 0.05	1.7 ± 0.1	2.6 ± 0.2	2.7 ± 0.2	2.5 ± 0.2
9	2.60 ± 0.05	2.1 ± 0.1		2.9 ± 0.1	2.8 ± 0.1
10	2.20 ± 0.05	2.0 ± 0.1	3.8 ± 0.2	4.0 ± 0.1	
11	2.6 ± 0.1		3.5 ± 0.2	3.7 ± 0.1	
12	2.8 ± 0.2		3.1 ± 0.3	3.3 ± 0.2	
13	2.7 ± 0.2		3.0 ± 0.2	3.0 ± 0.2	

[a] We report threshold energies (E_T) for each isomer of $SmSi_n^-$ that was observed. Since presently it is not known which of the two is lower in energy as a neutral species, the EA_a of those particular cluster compositions cannot be estimated without ambiguity.

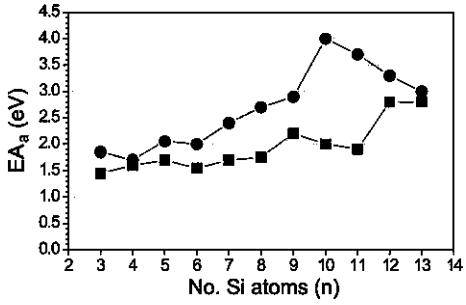

Figure 6. EA_a vs the number of silicon atoms, *n*, for prototypical members of category A, $EuSi_n$ (■), and category B, $HoSi_n$ (●).

In particular, the minimum size of the silicon cluster that fully encapsulates a Ln atom would be of interest from the perspective of potential applications. Such a cluster would be a unique building block for assembling magnetic, metal−silicon cluster materials. In the earlier study of the $TbSi_n^-$ system, a sudden decrease of the clusters' reactivity toward water at $n = 10$ was interpreted as marking the full encapsulation of the Tb atom. Correspondingly, a dramatic increase in the adiabatic electron affinity (EA_a) of $TbSi_{10}^-$ (3.60 eV) relative to $TbSi_9^-$ (2.20 eV) was observed as well.[28,29] Since the first peak in the photoelectron spectra of $LnSi_n^-$ cluster anions likely corresponds to the transition from the ground electronic state of the anion to the ground electronic state of its corresponding neutral, this transition provides an estimate of the EA_a of $LnSi_n$ species. The onset of the photoelectron intensity of the first peak was used to estimate the EA_a values of $LnSi_n$ clusters. For the $LnSi_n$ clusters, Ln = Ho, Pr, Sm, Yb, these are tabulated as a function of the number of silicon atoms, *n*, in Table 1. Data on EA_a values for $EuSi_n$, $GdSi_n$, and $TbSi_n$ have been previously published elsewhere.[26−29] The trends in EA_a values vs cluster size fall into one of two categories just as did the photoelectron spectra from which they were extracted (excluding Sm, whose dual behavior confines it to one or the other or sometimes both depending on the size *n*). The dependency of EA_a on *n* is plotted in Figure 6 both for a representative of category A, i.e., $EuSi_n$, and for a representative of category B, i.e., $HoSi_n$. In the case of the category B representative, the plot shows a large increase of the EA_a value of the $HoSi_{10}$ cluster compared to that of $HoSi_9$ (4.0 ± 0.1 and 2.9 ± 0.1 eV, respectively). A similarly dramatic increase, albeit at slightly larger cluster size, is observed in the case of a category A prototypical system, $EuSi_n$. There, the EA_a jumps from a low value of 1.9 ± 0.1 eV for $EuSi_{11}$ to a maximum of 2.8 ± 0.2 eV in the case of $EuSi_{12}$. Analogous observations were in previous work ascribed to the complete encapsulation of the lanthanide atom at those particular cluster sizes.[26,28,29] However, recent studies suggest that the increased electron affinities of $n = 10$ and $n = 12$ in the $Ln^{III}Si_n$ and $Ln^{II}Si_n$ series, respectively, are more likely due to an inherent electronic stabilization of those particular clusters, rather than the lanthanides' encapsulation. The latter is expected to occur when the size of the silicon cage swells to approximately 20−25 atoms.[27,47]

By focusing on the photoelectron spectra of $LnSi_n^-$ clusters belonging to the same category, one notices, upon closer inspection that their spectral features undergo small, but systematic shifts in EBE values. These shifts are reflected in slightly different estimates of EA_a values for $LnSi_n^-$ clusters in the same category (see Table 1). Since for a given *n* the only difference between these particular systems lies in the nature of the lanthanide atom, variations can be attributed to differences in the electronic structures between lanthanide atoms. Specifically, we postulate that the observed differences are due to the different electron affinities of the lanthanide atoms. Thus, one could use the existing data on $LnSi_n^-$ systems to estimate the relative electron affinities of lanthanide atoms. To better quantify the observed spectral shifts, we utilized the peak centers of prominent transitions. Since the differences vary for different *n* values, an average of all studied systems was taken for the final estimate. In principle, only elements from the same category may be compared in such a way. Fortunately, however, $SmSi_n^-$ systems link the two categories and thus allow the smaller clusters ($n \leq 10$) to be compared to category A, and the larger ones ($n = 7, 11, 12, 13$) to category B, thereby serving as a common reference point for both series. Relative values of electron affinities obtained in this manner are presented in Table 2. In spite of a significant statistical error, two conclusions can be reached. First, the electron affinities of all studied lanthanides appear to fall within 0.2 eV of each other. Second, with the exception of Tb, electron affinities generally increase when moving to heavier members of the lanthanide series. While several experimentally determined values of EA_a have been reported for lanthanide atoms, there is broad inconsistency among them, and it is hoped that the perspective offered here can contribute to unraveling this knotty problem.[48−50]

Conclusion

Anion photoelectron spectroscopic study of $LnSi_n^-$ systems (Ln = Eu, Yb, Gd, Ho, Pr, Sm, Tb;[28,29] $3 \leq n \leq 13$) has

(47) Koyasu, K.; Atobe, J.; Furuse, S.; Nakajima, A. *J. Chem. Phys.* **2008**, *129* (21), 214301.

Table 2. Estimated *Relative* Adiabatic Electron Affinities, rEA_a, of the Studied Lanthanides[a]

lanthanide atom	rEA_a (eV)
Pr	-0.05 ± 0.10
Sm	-0.04 ± 0.05
Eu	-0.02 ± 0.05
Gd	0.00
Tb	-0.10 ± 0.05
Ho	0.07 ± 0.05
Yb	0.05 ± 0.20

[a] All values are reported relative to that of Gd.

revealed that, at a particular size n, these clusters possess electronic structures (spectral patterns) that fall into one of two categories. These in turn correlate with the most common oxidation state that a particular lanthanide adopts in its compounds. We therefore conclude that, just as in those compounds, the lanthanides in Ln−silicon clusters exist either in a nominal +2 (Eu, Yb, Sm) or in a nominal +3 (Gd, Ho, Pr, Tb, Sm) oxidation state. By knowing the most commonly adopted oxidation states of the remaining lanthanide atoms, we can furthermore predict the likely electronic structures of the other $LnSi_n^-$ systems. For example, we speculate that La, Pm, and Er likely resemble the +3 systems, Dy resembles the +2 systems, and Tm and Nd are probably borderline examples resembling Sm, which exhibits +2 oxidation state in small clusters ($n \leq 10$) and +3 in larger clusters ($n \geq 7$). Since the f-electrons in the lanthanide atoms of these Janus-like systems are "on the fence" in regard to affecting their oxidation states, these systems may serve as especially sensitive benchmarks for development of new theoretical approaches that are capable of dealing with the highly correlated motion of f-electrons in lanthanides. Namely, the Ln atoms in such $LnSi_n^-$ systems not only undergo a transition from one oxidation state to the other at a particular size n, but also only exist in one or the other oxidation state rather than in some intermediate state. This binary behavior is nicely demonstrated by the $SmSi_{10}^-$ cluster, which exists in two different isomeric forms. In one, samarium adopts the +2 and in the other the +3 nominal oxidation state. This observation contrasts with usual chemical intuition, where the system would be expected to adopt some hybridized electronic structure with an intermediate oxidation state. The quantumlike behavior of these systems, where an electron can be either entirely located on the lanthanide atom or fully donated to the cage, closely resembles that of prototypical ionic systems. Formally therefore, the Ln(II) and Ln(III) atoms in silicon clusters may more accurately be described as Ln^{2+} and Ln^{3+}, respectively. The resulting $Ln^{2+/3+}(Si_n)^{2-/3-}$ neutral clusters would thus represent the basic unit of a Zintl-like salt. One could imagine exploiting these clusters as building blocks of silicon-based, cluster-assembled materials that may exhibit interesting magnetic properties. The low oxidation numbers that lanthanides adopt in Ln−silicon clusters imply only limited involvement of f-electrons in bonding with their surroundings. Since these electrons do not appear to be significantly perturbed by the environment, it is likely that they remain unpaired, just as in an isolated Ln atom. Consequently, they could retain significant portions of their magnetic moments even when enclosed by a silicon cage. The conclusions of this work may also be of relevance to the semiconductor industry, because the silicon cage enclosing a Ln atom crudely models the environment of a lanthanide atom implanted into a silicon crystal. Consequently, lanthanides doped into a silicon matrix would be expected to remain in a low oxidation state with f-electrons residing mainly on the lanthanide. While interactions with the crystal lattice may perturb them only slightly, they are likely to remain unpaired. Thus, implantation of these elements into a silicon substrate could present a shortcut to magnetic silicon-based materials that may find potential use in the nascent field of spintronics.

Acknowledgment. We appreciate insightful discussions with Dr. Atsushi Nakajima as well as with Dr. Peter Lievens and his student Nele Veldeman, all of whom gave us valuable advice during our efforts to develop the two-laser vaporization source employed in this study. We are very grateful to Dr. Bryan Eichhorn, whose insights into inorganic chemistry helped us in writing a well-rounded paper. We also enjoyed stimulating conversations with Dr. Shiv Khanna and Dr. Puru Jena, whose ideas motivated this work. We also acknowledge Dr. Mark Knickelbein, with whom we exchanged many fruitful experimental ideas. We furthermore thank the Division of Materials Sciences and Engineering, Office of Basic Energy Sciences, U.S. Department of Energy, for support of this work under Grant Number DE-FG02-09ER46558.

JA805205R

(48) Andersen, H. H.; Andersen, T.; Pedersen, U. V. *J. Phys. B: At., Mol. Opt. Phys.* **1998**, *31*, 2239.
(49) Davis, V. T.; Thompson, J.; Covington, A. *Nucl. Instrum. Methods Phys. Res., B* **2005**, *241*, 118.
(50) Nadeau, M.-J.; Garwan, M. A.; Zhao, X. L.; Litherland, A. E. *Nucl. Instrum. Methods Phys. Res., B* **1997**, 521.